ORIGINAL RESEARCH

# Anti-Inflammatory Effects of the 35kDa Hyaluronic Acid Fragment (B-HA/HA35)

XiaoXiao Jia[1,2,]*, Ming Shi [iD][3,]*, Qifei Wang[1,2], Jessica Hui[4], Joshua Hui Shofaro[1,2], Ryenchindorj Erkhembayar[5], Mizhou Hui[1,2], Chenzhe Gao[1], Munkh-Amgalan Gantumur[1]

[1]College of Life Science, Northeast Agricultural University, Harbin, People's Republic of China; [2]College of Veterinary Medicine, Qingdao Agricultural University, Qingdao, People's Republic of China; [3]School of Life Science and Technology, Harbin Institute of Technology, Harbin, People's Republic of China; [4]Center for Cancer Cell Therapy, Stanford Cancer Institute, Stanford University School of Medicine, Stanford, CA, USA; [5]Department of International Cyber Education, Graduate School, Mongolian National University of Medical Sciences, Ulaanbaatar, Mongolia

*These authors contributed equally to this work

Correspondence: Mizhou Hui; Munkh-Amgalan Gantumur, Email huimizhou@163.com; mnkh.calm@gmail.com

**Background:** Hyaluronic acid (HA) and HA fragments interact with a variety of human body receptors and are involved in the regulation of various physiological functions and leukocyte trafficking in the body. Accordingly, the development of an injectable HA fragment with good tissue permeability, the identification of its indications, and molecular mechanisms are of great significance for its clinical application. The previous studies showed that the clinical effects of injectable 35kDa B-HA result from B-HA binding to multiple receptors in different cells, tissues, and organs. This study lays the foundation for further studies on the comprehensive clinical effects of injectable B-HA.

**Methods:** We elaborated on the production process, bioactivity assay, efficacy analyses, and safety evaluation of an injectable novel HA fragment with an average molecular weight of 35 kDa (35 kDa B-HA), produced by recombinant human hyaluronidase PH20 digestion.

**Results:** The results showed that 35 kDa B-HA induced human erythrocyte aggregation (rouleaux formation) and accelerated erythrocyte sedimentation rates through the CD44 receptor. B-HA application and injection treatment significantly promoted the removal of mononuclear cells from the site of inflammation and into the lymphatic circulation. At a low concentration, 35 kDa B-HA inhibited production of reactive oxygen species and tumor necrosis factor by neutrophils; at a higher concentration, 35 kDa B-HA promoted the migration of monocytes. Furthermore, 35 kDa B-HA significantly inhibited the migration of neutrophils with or without lipopolysaccharide treatment, suggesting that in local tissues, higher concentrations of 35 kDa B-HA have antiinflammatory effects. After ^{99m}Tc radiolabeled 35 kDa B-HA was intravenously injected into mice, it quickly entered into the spleen, liver, lungs, kidneys and other organs through the blood circulation.

**Conclusion:** This study demonstrated that the HA fragment B-HA has good tissue permeability and antiinflammatory effects, laying a theoretical foundation for further clinical studies.

**Keywords:** hyaluronic acid, 35kDa hyaluronic acid fragment, B-HA/HA35, molecular weight, inflammation, inflammatory cells, reactive oxygen species, injection safety

## Introduction

Hyaluronic acid (HA) consists of repeating units of N-acetylglucosamine and glucuronic acid. HA and HA fragments are present in all tissues of the human body, providing lubrication, cushioning, elasticity, and tissue water retention. There are approximately 15 grams of HA and HA fragments in a 70 kg human; however, HA and HA fragments in the elderly are significantly reduced. The half-life of HA in the human body is 15 hours. It is estimated that one-third of the HA in the human body undergoes a daily renewal process of degradation and resynthesis, ie, a state of coexistence of HA and HA fragments.[1–3] Whilst existing as a high molecular weight polymer ($>10^6$ kDa) under normal conditions, HA can become degraded in response to various pathogenic events resulting in the generation of low molecular weight fragments.[4] HA fragments have the capacity to invoke both an

**209**

inflammatory response and induce synthesis of tissue degrading enzymes. These effects are mediated through HA cell surface receptors CD44 and/or toll-like receptor (TLR)-4, with subsequent activation of NF-κB.[5] Specifically, HA and HA fragments with different molecular weights interact with a variety of human body receptors, including lymphatic vessel endothelial hyaluronan receptor 1 (LYVE-1), CD44, HA-mediated motility receptor (RHAMM), Siglec-9, toll-like receptor (TLR) 2, HA-receptor for endocytosis (HARE), cell migration-inducing and hyaluronan-binding protein (CEMIP), and transmembrane protein 2 (TMEM2).[6–8] HA and HA fragments are involved in the regulation of leukocyte trafficking (neutrophils, macrophages, dendritic cells (DCs), T cells, and B cells) and the secretion of inflammatory cytokines by leukocytes (neutrophils, macrophages, DCs, T cells, B cells, and microglia).[7–11] HA and HA fragments have the potential to be effective drugs for the clinical treatment of pain, redness, swelling, inflammatory pain, and inflammatory diseases,[12–23] may regulate tumor immunity and be used to treat tumors,[24–28] and may also play an important role in the treatment and prevention of cardiovascular and cerebrovascular diseases.[29,30] HA and HA fragments indirectly affect leukocyte trafficking and leukocyte production of reactive oxygen species (ROS) via erythrocytes and the erythrocyte receptor CD44.[31–34] The life span of naked mole-rats is nearly 30 years, which is 10 times longer than that of normal rats. Six percent of the body weight of naked mole-rats is HA and HA fragments, and naked mole-rats do not suffer from cancer or serious disease, with no visible signs of aging, are insensitive to pain and have little subcutaneous adipose tissue.[35–40] These features of naked mole-rats support that HA and HA fragments may exert comprehensive anti-aging, anti-cancer, anti-tissue damage, anti-inflammatory, analgesic and lipolytic actions through various types of HA receptors. In addition, knocking out the genes that express hyaluronidase, HA synthase, and HA receptors in mice results in developmental abnormalities and functional changes, suggesting that HA and HA fragments have a beneficial therapeutic effect on the human body.[36–44]

Human hyaluronidase PH20 is a sperm acrosome hyaluronidase produced in male testes and is also produced in the female breast.[45–47] PH20 contained in human colostrum can cleave human high molecular HA to produce a 35 kDa HA fragment (HA35 or B-HA), which has anti-inflammatory properties in the skin mucosa.[18–23] Glycosylated recombinant human PH20 produced using Chinese hamster ovary (CHO) cells can be used for subcutaneous infusions, the subcutaneous administration of immunoglobulins and the subcutaneous administration of therapeutic antibodies when the PH20 purity is higher than 98.5%.[45,46] This recombinant human hyaluronidase PH20 is different from that extracted from bovine testis, does not require a skin sensitivity test, and does not induce human neutralizing antibody production.[46,48] Therefore, it is of important clinical significance to develop an injectable HA fragment with good tissue permeability using recombinant human PH20 and to further clarify the comprehensive effects of 35 kDa HA fragments on the above mentioned receptors in different tissues and organs after absorption. This paper reports a production method for injectable B-HA with an average molecular weight of 35 kDa and excellent permeability to human tissues, a method for molecular weight detection, and a method for erythrocyte and receptor activity detection and the results of studies of the level and functions of freshly extracted human leukocytes, tissue absorption and distribution in mice, and the safety of intravenous injection in dogs. This paper used freshly extracted human leukocytes to approximate a human clinical study to reveal the therapeutic effects of different concentrations of 35 kDa B-HA. Specifically, this study investigated the effects of low concentrations of 35 kDa B-HA on neutrophils and monocytes (mainly lymphocytes and a small amount of macrophage precursors, ie, monocytes) in blood and connective tissues with low concentrations of HA and HA fragments. We also examined the effects of topical high concentrations of 35 kDa B-HA on neutrophils and monocytes in lymphoid and brain tissues with high concentrations of HA and HA fragments.[49–51] The above studies showed that the clinical effects of injectable 35kDa B-HA in humans result from B-HA binding to multiple receptors in different cells, tissues, and organs. This study lays the foundation for further studies on the comprehensive clinical effects of injectable B-HA in humans.

## Materials and Methods
### Cells, Expression Vector and Experimental Samples
CHO and CHO-S cells and the pMH3 expression vector plasmid were obtained from Huihui Biotechnology, China. Forearm venous blood was obtained from a total of 12 healthy volunteers, aged 24±4 years old. The venous blood of beagle dogs, BALB/c mice, Inner Mongolian goats and Inner Mongolian cattle was provided by the Veterinary Hospital

of Qingdao Agricultural University, China. The documented review and approval from a formally constituted review board (Ethics committee of Qingdao Agriculture University) as well as the written informed consent of all the 12 volunteers in accordance with the Declaration of Helsinki were obtained for collection of all the human blood samples and experimentation of the beagles, mice, goats, and cattle.

## Experimental Reagents

The experimental reagents used in this study included the following: injection grade 1600 kDa HA, 300 kDa HA and 24 kDa HA fragments (Freda, China); 60 kDa HA fragments (Shandong Liyong Biotechnology Co., Ltd., China); fetal bovine serum (FBS) (Zhejiang Tianhang Biotechnology Co., Ltd., China); penicillin (HyClone, USA); anti-human CD44 antibody and non-specific rabbit IgG antibody (Abcam, UK); Cy5.5 fluorescent dye, lipopolysaccharide (LPS), agarose and phorbol ester (PMA) (Solarbio Life Sciences, China); RPMI-1640 medium, PBS buffer, and carboxylate modified polystyrene (Fluorescent Particles) (Sigma-Aldrich, USA); human neutrophil isolation kit (Haoyang Huake, China); tumor necrosis factor α (TNF-α) enzyme-linked immunosorbent assay (ELISA) kit (R&D Systems, USA); Human HAase ELISA Kit (Shanghai Enzyme-linked Biotechnology Co., Ltd., China); and SDS-PAGE gel preparation kit (CoWin Biosciences, China).

## Expression of Recombinant Human Hyaluronidase PH20

According to the process described by Jia et al,[52] the cDNA of recombinant human hyaluronidase PH20 was inserted into the GC-rich empty pH3 expression vector to construct the pMH3-pH20 expression vector. pMH3-PH20 was transfected into CHO-S cells to generate a cell line with high PH20 expression. This cell line was amplified and cultured on a large scale in a jet-type animal cell reactor. The collected PH20 was purified in 4 steps by Q Sepharose fast flow (QFF) column, phenyl HP hydrophobic column, CHT type I ceramic hydroxyapatite column and SP HP cation exchange column.

## Agarose Gel Electrophoresis

All samples were diluted to a final concentration of 5mg/mL. Then, diluted samples and standards were mixed 4:1 with loading buffer. Electrophoresis was conducted at 80 V for 20 min. The gel was distained for 2 h, until the sample band was clearly visible, and the 1% agarose gel was photographed in the bright place.

## Eighteen-Angle laser scattering Gel Permeation Chromatography (MALLS-GPC)

Online MALLS-GPC combined with a refractive index detector (RID) was used to analyze the molecular weight of the samples. (1) Chromatographic conditions were as follows: high-performance liquid chromatography (HPLC) (with an RI detector); Shodex SB-804 HQ gel column ($\Phi$8 mm × 300 mm); mobile phase – 0.02% sodium azide sodium; flow rate – 1 mL/min; injection volume – 100 μL; temperature – 40 °C; and detector – RID and MALLS. (2) To determine the relative molecular mass of each sample, an appropriate amount of sample was weighed to prepare a 1 mg/mL polysaccharide solution, which was filtered for HPLC analysis. (3) For the molecular mass distribution, the mass concentration and light scattering intensity at different angles were measured by RID and a laser detector, respectively. The refractive index increment (dn/dc) value was 0.138. The molecular mass distribution map of the test samples was obtained using the data processing software ASTRA.

## Erythrocyte Aggregation (Rouleaux Formation) Detection (Including a CD44 Blocking Study)

HA fragments with different molecular weights and HA materials (Supplementary Table 1) were mixed with human venous blood at a ratio of 1:2, with final concentrations of 1.2%, 0.6%, 0.3%, 0.15%, 0.075%, and 0.0375%. A red blood cell smear was prepared, and erythrocyte aggregation (rouleaux formation) was observed under a microscope.

Anti-human CD44 antibody (0.5 mg/mL), control nonspecific rabbit IgG antibody (0.5 mg/mL) or PH20 (27,000 U/mL) was mixed with human venous blood at final concentrations of 10 μg/mL, 10 μg/mL, and 1927 U, respectively. After incubation at 37 °C for 25 min, B-HA was added to prepare red blood cell smears, which were observed under a microscope.

HA fragments of different molecular weights and raw HA materials (Supplementary Table 1) were mixed with venous blood from different animals (rats, beagle dogs, sheep and cattle) at a ratio of 1:2 at final concentrations of 1.2%, 0.6%, 0.3%, 0.15%, 0.075% and 0.0375%, respectively. Red blood cell smears were prepared and observed under a microscope.

## Determination of the Degree of Variation in the Molecular Weight of Different Batch Products Using the Erythrocyte Sedimentation Rate

Low-molecular-weight B-HA was mixed with freshly collected venous blood from humans, beagle dogs, and mice at a ratio of 1:2 at final concentrations of 0.15%, 0.11%, and 0.075%, respectively. A total of 400 µL of mixed blood was aspirated into a blood sedimentation tube and allowed to rest for 25 min. The blood sedimentation in the tube was measured to calculate the erythrocyte sedimentation rate.

## Tissue Distribution of $^{99m}$Tc-Labeled B-HA

$SnCl_2$ was used to reduce Tc(V) to $[TcOCl_4]^-$ and bind to the carboxyl groups of B-HA to form a $^{99m}$Tc-labeled B-HA stable compound ($^{99m}$Tc-B-HA). After purification by SEC-HPLC, $^{99m}$Tc-B-HA with purity greater than 98% was obtained. Purified $^{99m}$Tc-BH was intravenously injected through a preplaced catheter into healthy C57BL/6J mice (Jackson Laboratory, USA) aged 6–8 weeks. An iQID gamma camera was used to dynamically assess the distribution of $^{99m}$Tc-B-HA in whole-body tissues for 3 hours. After the collection of iQID images, blood, tissue and organ samples were collected from the mice for radiometric determination. The $^{99m}$Tc-B-HA distribution in the tissues and organs of mice was expressed as the percentage of the total injected dose (% ID/g).

## Inhibition of ROS Production by Human Blood Neutrophils Using B-HA

Neutrophils were obtained according to the instructions of a human venous blood neutrophil isolation kit. The neutrophils were resuspended in RPMI-1640 medium containing 10% FBS ($2 \times 10^6$ cells/mL). Cells were inoculated into 24-well plates (200 µL/well). DHR123 fluorescent dye (5 mM) was added, and the cells were incubated in the dark for 15 min at 37 °C. The 40 µg/mL B-HA, 40 µg/mL HA, or 5 nM PMA was added, and the cells were incubated in the dark for 40 min at 37 °C. Then, the cells were washed with precooled PBS twice and resuspended. Flow cytometry (FACS) was used to detect the amount of ROS produced by neutrophils. Venous blood was collected from 3 different volunteers each time.

## Detection of TNF-α by ELISA

TNF-α levels were measured using supernatants collected after PMA-induced ROS production by neutrophils. Detection of TNF-α in cell culture medium was performed using a TNF-α ELISA kit. The concentration of TNF-α was determined using a human enzyme-linked immunosorbent assay kit following the manufacturer's instructions.

## Effects of High Concentrations of B-HA on the Migration of Freshly Extracted Neutrophils and Monocytes

Neutrophils and monocytes were obtained by following the instructions of a human venous blood neutrophil isolation kit. The cells were resuspended in RPMI-1640 medium at $3 \times 10^8$ cells/mL. Agarose solution (0.8%) was mixed with RPMI-1640 (containing 20% FBS) in equal proportions. Subsequently, the neutrophil suspension was added at a ratio of 1:1 and incubated in the water bath at 37 °C. The neutrophil agarose mixture (2 µL) was pipetted into each well of a precooled 96-well plate. Gel droplets approximately 2 mm in diameter were formed and placed at 4 °C for 15 min. RPMI-1640 medium containing 1 µg/mL anti-CD44 antibody, 300 µg/mL B-HA, 300 µg/mL HA, 300 µg/mL B-HA+300 µg/mL HA, 1 ng/mL LPS, and 1 nM N-formyl-methionyl-leucyl-phenylalanine (fMLP) was prepared separately, and 100 µL of the prepared mixtures was added to each well after the agarose droplets in the wells had solidified. Four parallel trials were set up for each group. After incubation at 37°C for 3 hours, the cells were observed and photographed, and the migration area was calculated using Image J. Venous blood was collected from 3 different volunteers each time.

## Study on the Safety of the Intravenous Injection of B-HA in Beagle Dogs

Thirty beagle dogs received an intravenous injection of 100 mg/5 mL sterile B-HA solution, pH 6.5–7.5 (endotoxin <0.5 EU/5 mL), in the forelimbs twice. The responses of the beagle dogs during injection and after injection were observed.

## Subcutaneous Injection and Application of B-HA to Tissue Sections of the Beagle's Skin Wound Inflammation

Before starting the experiment, the beagle dogs were adapted to their environment for a week. At the beginning of the experiment, the animals were divided into 3 groups, each group of two. Experimental dogs were anesthetized by intramuscular injection of Zoletil®50 (5–11mg/kg).

The operating table was prone, fixed, and the back was sheared and disinfected. On the first day, two wounds (about 1.5 cm in length and 4 mm in depth) were cut in a symmetrical position on the left and right sides of the center line of the dog's back. The control group was performed without any treatment. In the B-HA and HA groups, B-HA and HA were applied to the wound twice a day at a concentration of 20 mg/mL. The duration of the experiment was 5 days. The Institutional Animal Care and Use Committee of Qingdao Agricultural University approved the protocol of this study. All experimental animal tests were carried out according to the 2016 China Laboratory Animal Standards and other related regulations in the Animal Welfare Law.

## Statistical Analyses

The data are expressed as the mean ± SD, and statistical analyses were performed using GraphPad Prism 6.0. The results were compared using group $t$-tests. $p > 0.05$(ns) was considered not statistically significant, $p < 0.05$(*) was considered statistically significant, and $p < 0.01$(**) and $p < 0.001$(***) were considered highly statistically significant.

# Results
## Methods for 35 kDa B-HA Production, Detection, and Quality Control

CHO cells were used to produce recombinant human PH20, which was purified in 4 steps using a Q Sepharose Fast Flow (QFF) chromatography column, a phenyl HP hydrophobic chromatography column, a CHT type I ceramic hydroxyapatite chromatography column, and an SP HP cation exchange chromatography column. Glycosylated recombinant PH20[43,44,48] with purity >98.5% was obtained (Figure 1A), and the specific activity was 56,802±508 IU/mg (n = 3). This recombinant human PH20 can be used to cleave injection-grade polymer HA raw materials to produce 35 kDa HA fragments (B-HA or HA35).[18–23,53–57]

Bioactive hyaluronic acid fragment HA35 of 35kDa was isolated from human colostrum. The B-HA production process, which had obtained a marketing permit in Mongolia, is described below. In a 40-L enzymolysis reactor, 140 mM NaCl, 1 mM MgCl solution, 1 g of injection grade HA (molecular weights ranging from 1200 to 1800 kDa) and 15,000 IU PH20 were added successively and mixed well, and samples were taken at different times during a 37 °C culture (Figure 1B). An optimum incubation time of 4 hours was determined. Residual PH20 in enzymatic digestion products was heat inactivated, and then, the products were filtered to remove bacteria. Endotoxin content, residual protein, residual nucleic acids, cultured bacteria and glucuronic acid content were assessed. The average molecular weight of B-HA products from 6 different batches was 35±8 kDa, with a coefficient of variation (CV) of 22% (n = 6) by MALLS-GPC determination (Figure 2A). These findings are consistent with the molecular weight of B-HA extracted from human colostrum.[46,47,52–54] Based on the molecular weight distribution results, 92.75±2.42% of B-HA was between 10 and 70 kDa, and 96.92±2.34% of B-HA was between 10 and 100 kDa (Figure 1C and D), with a relatively small distribution range. The 35 kDa B-HA was completely filtered using a 0.22 μm filter membrane, indicating good tissue permeability. Compared to HA fragments produced by physical and chemical cleavage, B-HA had no structural and physicochemical damage. In comparison with HA fragments produced by enzymatic cleavage of hyaluronidase extracted from immunogenic animals and insects or produced from nonglycosylated microorganisms, the B-HA produced herein did not induce allergic reactions,[46] did not require skin sensitization tests and was more suitable for the manufacture of injections.
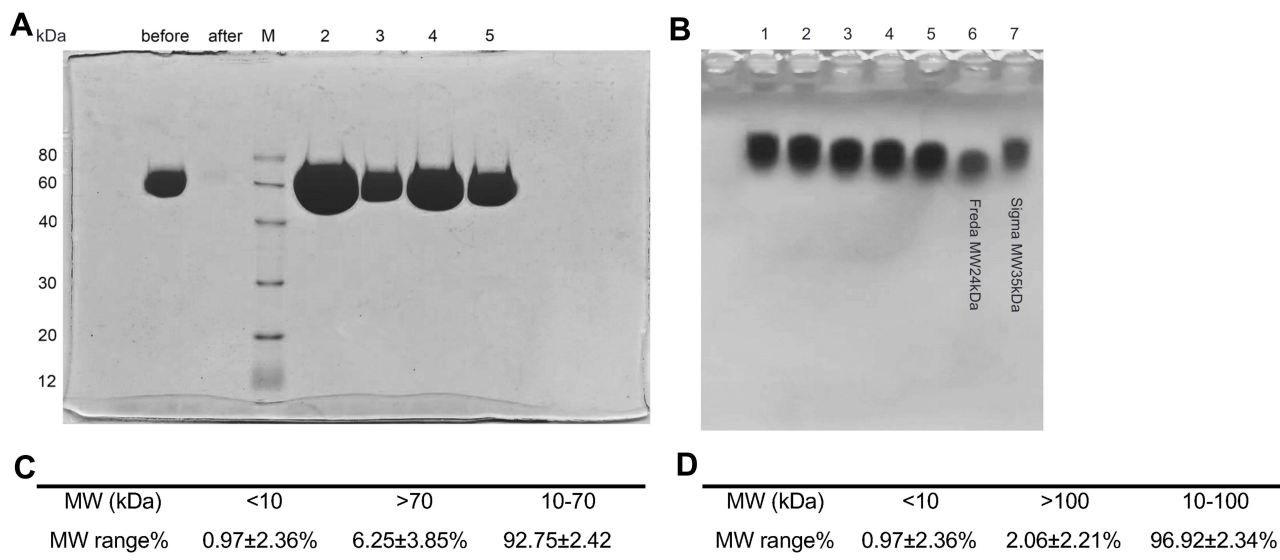
**Figure 1** Determination of B-HA production conditions and measurement of the molecular weight distribution. (**A**) SDS-PAGE detection of purified recombinant human hyaluronidase PH20. (**B**) HA raw material and recombinant human hyaluronidase PH20 were cultured for 30 min (lane 1), 1 hour (lane 2), 2 hours (lane 3), 3 hours (lane 4) and 4 hours (lane 5). The samples were electrophoresed for 20 min. Lane 6 and lane 7 were standards for 24 kDa and 35 kDa HA fragments, respectively. (**C**) Molecular weight distribution results, 10–70 kDa for 6 batches of B-HA products detected by MALLS-GPC. (**D**) Molecular weight distribution results, 10–100 kDa for 6 batches of B-HA products detected by MALLS-GPC.

The results in Table 1 and Figure 2 indicated that low molecular weight HA fragments at a range of 24, 35, and 60 kDa bind to human erythrocyte cell surfaces through CD44 and trigger erythrocyte aggregation (rouleaux formation). It was indicated that the minimum concentration which triggers erythrocyte aggregation (rouleaux formation) was positively correlated with the molecular weight of the low molecular weight HA fragments. This positive correlation could be used to measure the molecular weight of an average molecular weight of HA fragments. The 24 kDa HA fragments had the best tissue penetration capability and the worst cell surface or CD44 binding capability. The 60 kDa HA fragments had the worst tissue penetration capability and the best cell surface or CD44 binding capability. The 35 kDa HA fragments had both the tissue penetration capability and the cell surface or CD44 binding capability in the middle. Therefore, this study chose the 35 kDa HA fragments to serve as the raw material for B-HA injection.

Findings have shown that different molecular weights of B-HA and HA induce human erythrocyte aggregation (rouleaux formation) (Figure 2B–E). The minimum percent concentration that induced human erythrocyte aggregation (rouleaux formation) was negatively correlated with the molecular weight of B-HA within a certain range (Table 1, Figure 2F). The minimum percent concentrations of HA fragments with average molecular weights of 24 kDa, 35 kDa, and 60 kDa induced erythrocyte aggregation (rouleaux formation), which were 0.6%, 0.15%, and 0.0375%, respectively. The use of an anti-human CD44 antibody blocked 0.15% of 35 kDa B-HA-induced erythrocyte aggregation (rouleaux formation) (Figure 2B–E), suggesting that this phenomenon induced by 35 kDa B-HA is mediated by the erythrocyte surface molecule CD44. Furthermore, low-molecular-weight B-HA did not induce erythrocyte aggregation (rouleaux formation) in cattle and sheep, only high-molecular-weight HA induced this phenomenon (Supplementary Table 2 and 3), and there was species variability (Supplementary Table 2–5).

In addition to inducing erythrocyte aggregation (rouleaux formation), low-molecular-weight B-HA also induced an increase in the erythrocyte sedimentation rate in humans, dogs and mice (Supplementary Table 6–8). The erythrocyte sedimentation rate can be used as a quality control method to quantify the degree of molecular weight variation between batches of low-molecular-weight HA products. The biological significance of this phenomenon has been further investigated.[58,59]

## Tissue Distribution of Injectable B-HA

Five minutes after the intravenous injection of ^{99m}Tc-B-HA in mice, ^{99m}Tc-B-HA was rapidly distributed to the spleen and liver, followed by the lungs. Dynamic imaging demonstrated that ^{99m}Tc-B-HA was rapidly cleared in the blood, with
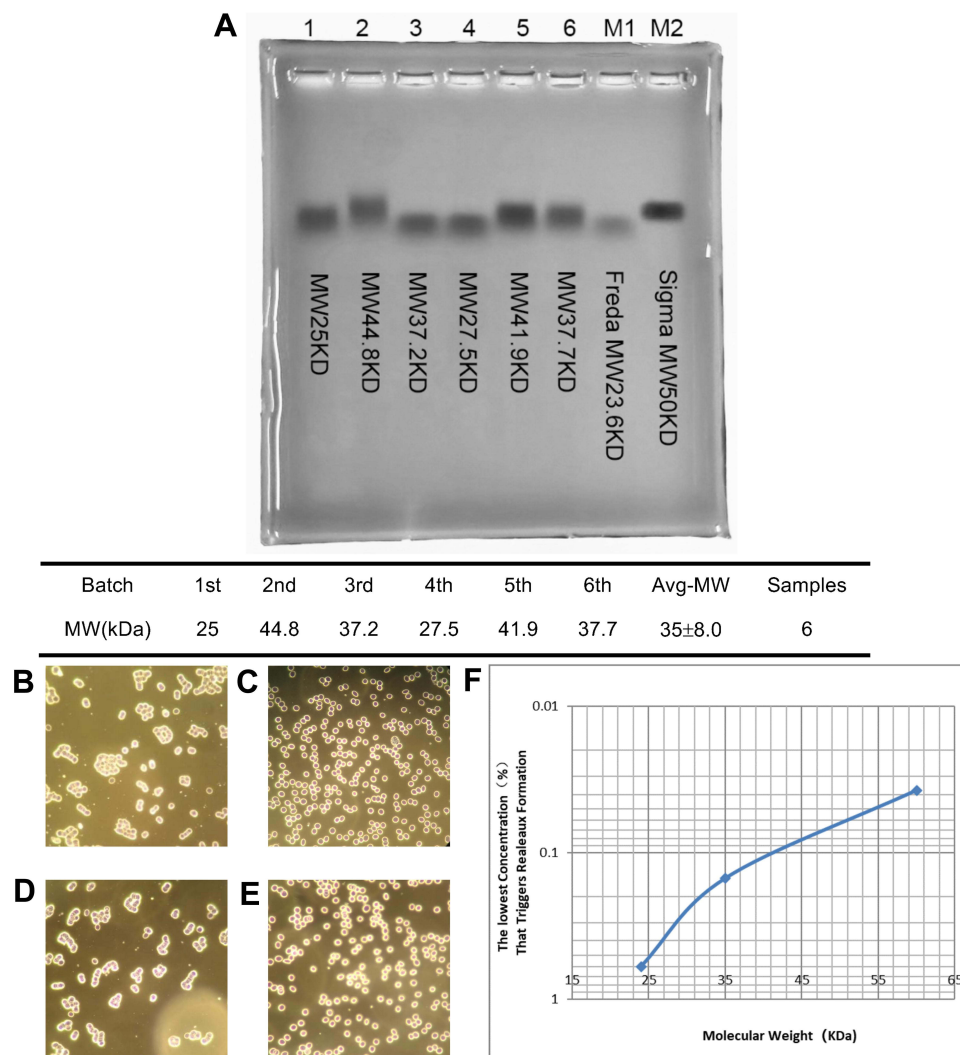
**Figure 2** 35 kDa B-HA causes erythrocyte aggregation (rouleaux formation). (**A**) 35 kDa B-HA was detected by gel electrophoresis. The molecular weights of 6 different batches of B-HA were obtained from the MALLS-GPC molecular weight measurement results. (**B**) B-HA at a final concentration of 0.15% induced human erythrocyte aggregation (rouleaux formation). (**C**) Anti-human CD44 antibody (10 μg/mL) inhibited B-HA-induced human erythrocyte aggregation (rouleaux formation). (**D**) Nonspecific rabbit IgG antibody (10 μg/mL) did not completely inhibit B-HA-induced human erythrocyte aggregation (rouleaux formation). (**E**) Recombinant human hyaluronidase PH20 (1927 U/mL) inhibited B-HA-induced human erythrocyte aggregation (rouleaux formation). (**F**) The semilogarithmic curve for the negative correlation between the minimum percent concentration of B-HA with different molecular weights that induced human erythrocyte aggregation (rouleaux formation) and the molecular weight.

a blood half-life of approximately 5 min (Figure 3). B-HA can be easily filtered by a 0.22um filter. Combined with the rapid distribution in the spleen, B-HA has good tissue permeability. The injected ^{99m}Tc-B-HA is absorbed subcutaneously and then transported to the lymphatic system for absorption, binds to the HA receptor LYVE-1 and promotes the migration and transport of mononuclear cells into the interstitial fluid of inflamed areas.[1–3,12,13,45,60,61] Unpublished data were also consistent with previously published studies, ie, HA and B-HA were rapidly absorbed by the lymphatic system after subcutaneous injection and were absorbed and transported to tissue fluid in inflamed areas.[50,59,61] 99mTc-B-HA was distributed in the liver, suggesting that ^{99m}Tc-B-HA can rapidly enter into the liver via the hepatic HA receptor HARE.[9,10,62] ^{99m}Tc-B-HA was, to a certain extent, distributed in the bladder, indicating that ^{99m}Tc-B-HA was excreted in urine through the kidneys. There was little distribution in the blood, suggesting that ^{99m}Tc-B-HA in the blood was quickly absorbed by tissues to exert functions or undergo metabolism. The results of this study were basically consistent with previous studies,[50,59,60] thus laying the foundation for subsequent similar studies on tissue distribution and blood half-life in dogs or monkeys.

**Table 1** Minimum Percent Concentrations of HA and B-HA, with Different Molecular Weights, That Induced Human Erythrocyte Aggregation (Rouleaux Formation)

|  | Final conc | HA 24 kDa | B-HA 35 kDa | HA 60 kDa | HA 300 kDa | HA 1600 kDa |
|---|---|---|---|---|---|---|
| MW (kDa) |  | 24 | 35 | 60 | 300 | 1600 |
| MW range (kDa) |  | 10–40 | 10–70 | 40–90 | 200–400 | 1200–1800 |
| Erythrocyte aggregation | 1.20% | Yes |  |  |  |  |
|  | 0.60% | **Yes** |  |  |  |  |
|  | 0.30% | No | Yes | Yes | No* | Yes* |
|  | 0.15% | No | **Yes** | Yes | **Yes** | **Yes** |
|  | 0.08% | No | No | Yes | No | No |
|  | 0.04% | No | No | **Yes** | No | No |
|  | 0.02% | No | No | No | No | No |

**Notes**: The bold characters are the minimum concentrations of HA that induced human erythrocyte aggregation (rouleaux formation), and *Indicates severe cell deformation.

## Low Concentrations of 35 kDa B-HA Inhibited the Activity of Activated Neutrophils

Human neutrophils are inactivated in blood vessels under normal conditions, ie, they do not produce ROS, and they do not produce inflammatory damage inside the blood vessels. Human neutrophils are activated by inflammatory factors or chemokines released by inflammatory tissues and migrate to inflammatory tissues, and after activation, they not only act on invading pathogenic microorganisms but also participate in the pathological processes of inflammatory diseases. The results of an unpublished study indicated that low concentrations (20–40 μg/mL) of B-HA had no significant effect on the apoptosis, migration, and phagocytosis of freshly extracted human neutrophils. Therefore, this study further investigated the effect of low concentrations (40 μg/mL) of HA and B-HA on leukocyte activation (produced by ROS).
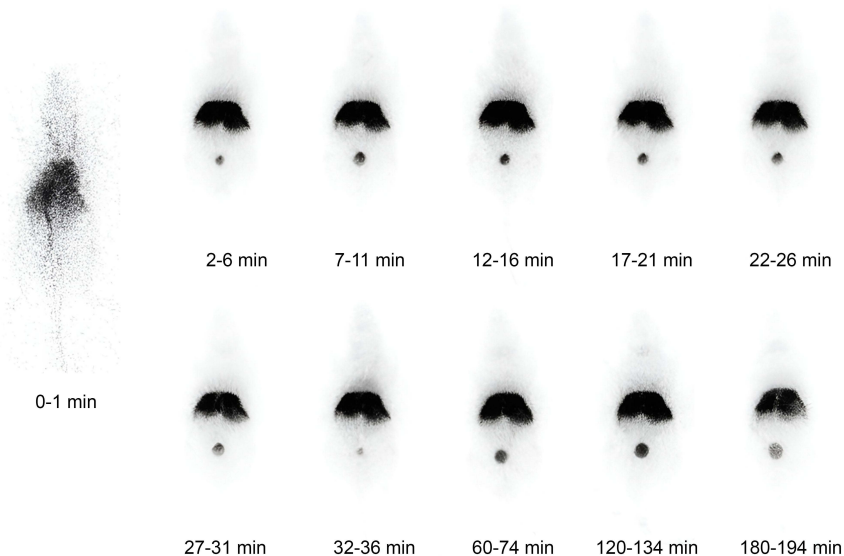
| Tissue | Blood | Heart | Lung | Liver | Spleen | Stomach | Small intestine | Large intestine | Kidney | Skin | Muscle | Salivary gland |
|---|---|---|---|---|---|---|---|---|---|---|---|---|
| Avg. | 0.565 | 0.241 | 1.376 | 44.003 | 11.929 | 0.976 | 0.719 | 0.289 | 1.082 | 0.122 | 0.049 | 0.877 |
| SD | 0.537 | 0.108 | 0.866 | 4.733 | 4.372 | 1.064 | 0.432 | 0.177 | 0.881 | 0.061 | 0.032 | 1.069 |
| Samples | 5 | 5 | 5 | 5 | 5 | 5 | 5 | 5 | 5 | 5 | 5 | 5 |

**Figure 3** Tissue distribution of $^{99m}$Tc-B-HA fragments. (**A**) iQID dynamic imaging of whole-body tissue distribution in mice after the intravenous injection of $^{99m}$Tc-B-HA (**B**) Statistics of the major distribution results after the intravenous injection of $^{99m}$Tc-B-HA.

**216**

Journal of Inflammation Research 2023:16

The results of the current study revealed that low concentrations of 35 kDa B-HA and 1600 kDa HA both inhibited PMA-induced ROS production by human neutrophils and that the inhibitory effects were basically the same (Figure 4A), suggesting that HA and B-HA act through common human neutrophilic receptors, ie, CD44 and Siglec-9, on blood cells.[57,58] We used recombinant human intestinal alkaline phosphatase, known to inhibit inflammation, and carbon-60 dissolved in grape seed oil to verify the reliability of the methods in this study.[63]

In addition, the level of TNF-α released from PMA-activated freshly extracted human neutrophils was significantly increased (P < 0.05). Low concentrations of both 35 kDa B-HA and 1600 kDa HA inhibited the release of TNF-α from PMA-activated human neutrophils (Figure 4B, P < 0.05). The results suggested that HA and B-HA had the same inhibitory effect on inflammatory factors released by neutrophils.

## Effects of High Concentration of 35 kDa B-HA on the Migration of Human Neutrophils and Monocytes

The results of this study showed that high concentrations (300 μg/mL) of 35 kDa B-HA and 1600 kDa HA promoted the migration of freshly extracted monocytes (mainly lymphocytes and a small amount of macrophage precursors, ie, monocytes) and that the combination of 35 kDa B-HA (300 μg/mL) with 1600 kDa HA (300 μg/mL) further promoted this effect. Anti-CD44 antibody, endotoxin LPS (1 ng/mL), and chemokine fMLP all promoted monocyte migration (Figures 5A and 6). This outcome indicates that the injection of B-HA into the lymphatic system with a relatively high concentration of HA further promotes monocyte migration and a return to circulating blood.

Furthermore, high concentrations of HA and 35 kDa B-HA had inhibitory effects on neutrophil migration under normal conditions, with a degree of action that was basically identical (Figure 5B). In the case of LPS induction, high concentrations of B-HA, HA, and the combination of the 2 significantly inhibited LPS-induced neutrophil migration (Figure 5C). These results suggested that HA and B-HA exhibited similar affinities and biological effects on HA receptors such as CD44 and Siglec-9. Anti-human CD44 antibody promoted neutrophil migration (Figure 5B). These results combined with the inhibition of neutrophil migration by dexamethasone (unpublished data) suggest that the topical use of high concentrations of injectable B-HA in human tissues (especially neural and lymphatic tissues with
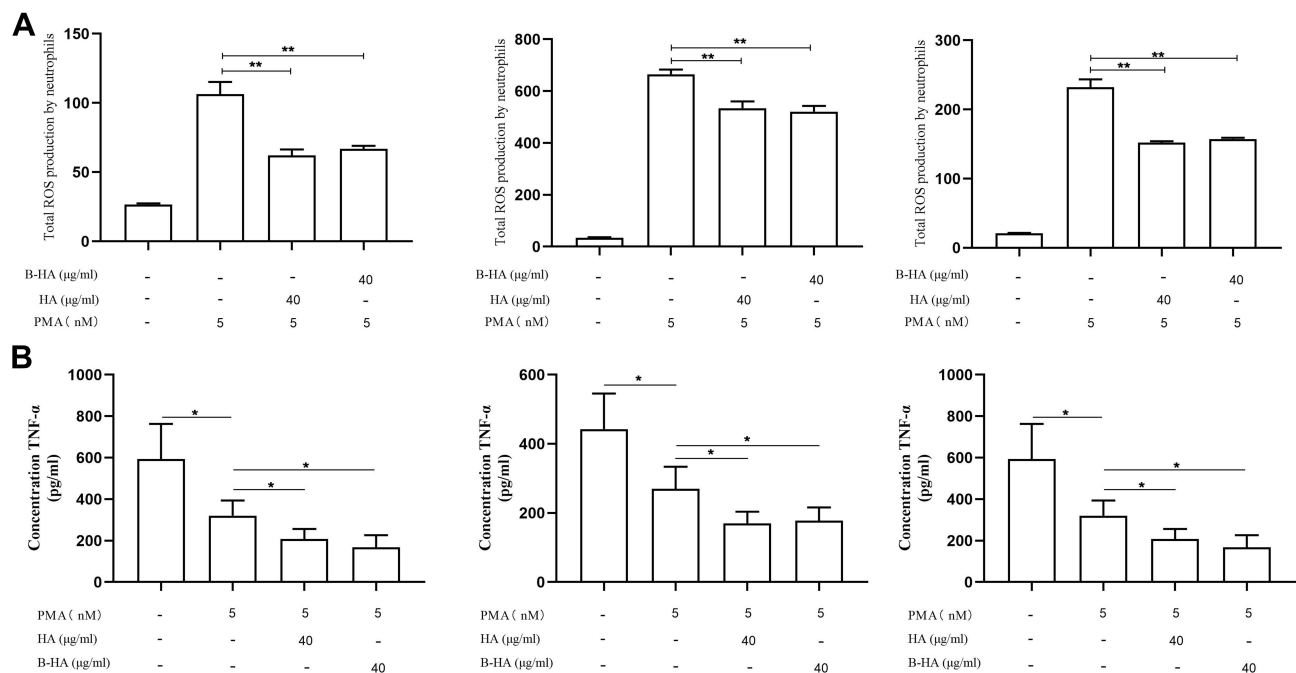


**Figure 4** 35 kDa B-HA inhibits the production of ROS and TNF-α by human neutrophils in blood vessels. (**A**) The inhibitory effects of low concentrations (40 μg/mL) of HA and 35 kDa B-HA on the production of ROS in freshly extracted human neutrophils. **\*\***Comparison between 2 groups, *p*<0.01 (n=4). (**B**) The inhibitory effect of low concentrations (40 μg/mL) of 35 kDa B-HA and 1600 kDa HA on the release of TNF-α by PMA-activated human neutrophils. *Comparison between 2 groups, *p*<0.05 (n=4).
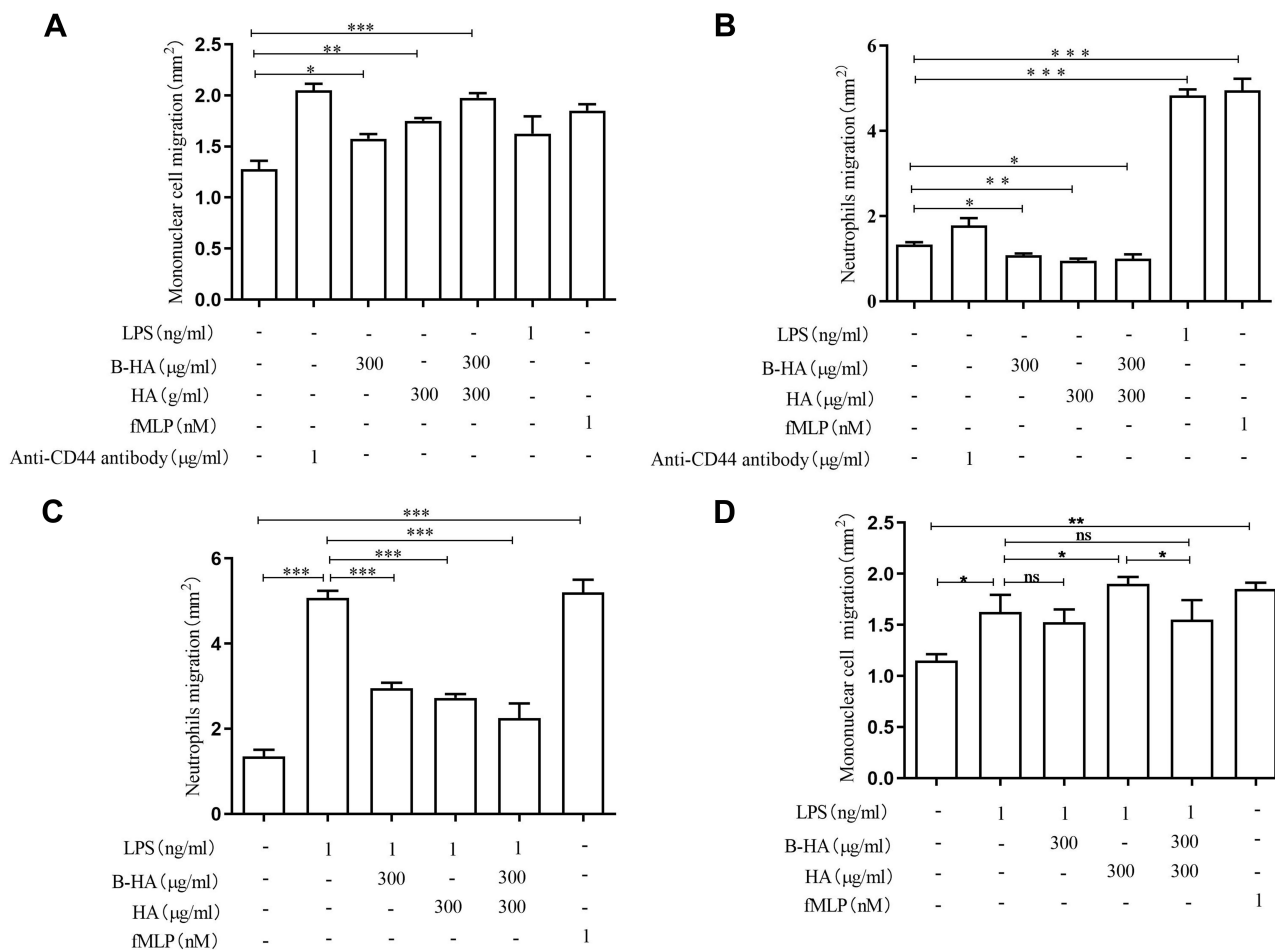
**Figure 5** Effects of high concentrations of B-HA on the migration of human neutrophils and monocytes. (**A**) High concentrations (300 μg/mL) of 35 kDa B-HA and 1600 kDa HA promoted the migration of monocytes; the combination of 35 kDa B-HA and 1600 kDa HA further promoted the migration of freshly extracted monocytes. Anti-human CD44 antibody, LPS, and fMLP all promoted monocyte migration. *Comparison between 2 groups $p<0.05$ (n=4); **Comparison between 2 groups $p<0.01$ (n=4); ***Comparison between 2 groups $p <0.001$ (n=4). (**B**) High concentrations (300 μg/mL) of B-HA, 1600 kDa HA, and the combination of B-HA and 1600 kDa HA all inhibited the migration of neutrophils. *Comparison between 2 groups, $p<0.05$ (n=4), **Comparison between 2 groups, $p<0.01$ (n=4). (**C**) High concentrations (300 μg/mL) of B-HA, HA, and the combination of HA and B-HA all significantly inhibited LPS (1 ng/mL)-induced neutrophil migration. LPS and fMLP promoted neutrophil removal. ***Comparison between 2 groups, $p<0.001$ (n=4). (**D**) High concentrations (300 μg/mL) of B-HA promoted LPS (1 ng/mL)-induced monocyte migration. *Comparison between 2 groups $p<0.05$ (n=4), **Comparison between 2 groups $p<0.01$ (n=4), ns comparison between 2 groups $p>0.05$ (n=4).

a high HA content) inhibited neutrophil migration and had an antiinflammatory effect. As seen in Figure 5D, both LPS and fMLP promoted neutrophil migration, indicating the reliability of the method used in this study. In general, high concentrations of B-HA and HA promoted the migration of monocytes and inhibited neutrophil migration in the presence and absence of LPS (Figures 5 and 6).

## Observation and Safety Study of Tissue Sections of Inflammatory Wounds Injected with B-HA

The skin of the dogs from the control group showed severe wound redness and swelling, accompanied by the outflow of pus, and the degree of wound healing was incomplete. Both the B-HA group and the HA group showed good wound healing, no redness, no pus outflow, and no obvious scab. Display of tissue section results, compared with the control group, the B-HA group had denser invasive connective tissue and less inflammatory cells. B-HA group had less fibrous tissue and granulation tissue than HA group (Figure 7).

In addition, 30 beagle dogs were also intravenously injected with sterile 35 kDa B-HA, pH 6.5–7.5, at a concentration of 100 mg/5 mL (endotoxin <0.5 EU/5 mL). The results of previous studies showed that high concentrations of B-HA, ie, greater than 0.15% (1500 μg/mL) and greater than 0.08% (800 μg/mL), caused erythrocyte aggregation and an elevated
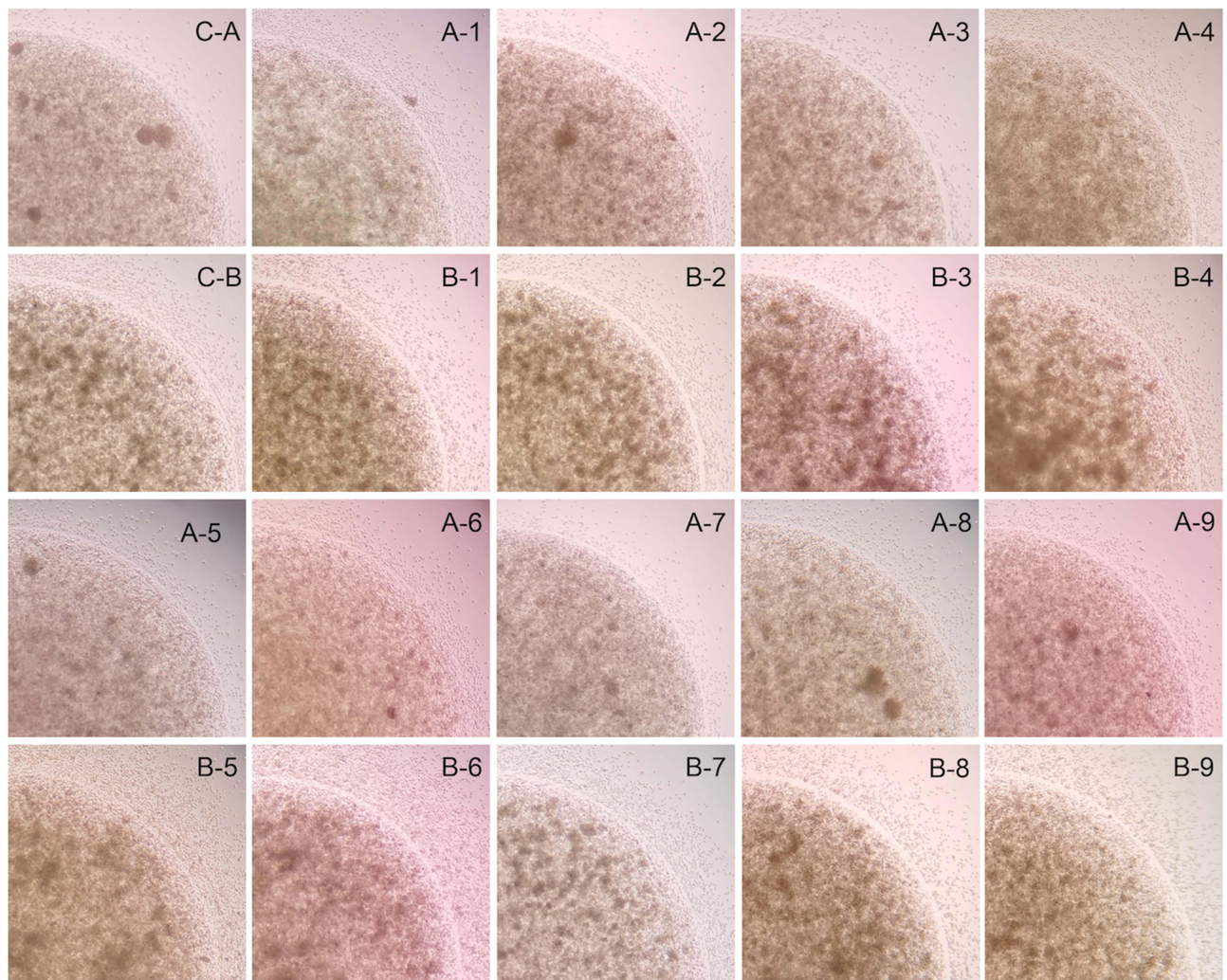
**Figure 6** Mononuclear cell and neutrophil migration from the inside of the gel droplet (FBS 5%) to the medium outside the gel droplet (FBS 10%). Microscope photo magnification is 120x. Microscope pictures are taken from the longest distance of cell migration. (**C**–Control, **A**–Mononuclear cell migration, **B**–Neutrophil migration, **1**–Anti-CD44 antibody 1μl/ml, **2**–B-HA 300μg/ml, **3**–HA 300μg/ml, **4**–B-HA+HA 300μg/ml, **5**–LPS 1ng/ml, **6**–fMlp 1nM, **7**–B-HA 300μg/ml+ LPS 1ng/ml, **8**–HA 300μg/ml+ LPS 1ng/ml, **9**–B-HA+HA 300μg/ml+ LPS 1ng/ml).

erythrocyte sedimentation rate. However, there was no local injection pain or blockage of blood vessels in beagle dogs during this experiment, and there was no struggle, avoidance or death caused by allergic reactions (Table S9). Accordingly, our findings suggested that the application of injectable B-HA is safe to use for clinical research.

## Discussion

This paper reports a method for the production of an HA/PH20-based injectable tissue-permeable B-HA with an average molecular weight of 35 kDa with no allergic reaction in humans. Exogenous or endogenous high molecular hyaluronic acid can be degraded into fragments of different molecular weights by hyaluronidase in vivo and penetrate into the tissue. HA interacts with multiple tissue receptors in vivo, including LYVE-1 (macrophages, DCs, T cells, and B cells), CD44 (erythrocytes, leukocytes and bone marrow cells), RHAMM (leukocytes, microglia, endothelial cells and muscle cells), Siglec-9 (neutrophils, monocytes, and DCs), TLR2 (macrophages, DCs, T cells, B cells, monocytes, and microglia), HARE (sinus endothelial cells of the liver, lymph nodes, and spleen), CEMIP (fibroblasts, epithelial cells, and multiple types of tumor cells) and TMEM2 (multiple types of tumor cells), which are involved in the regulation of multiple functions in the body[1,9,10,12–34] and play important roles in naked mole-rats.[35,36,64–68] However, HA is a very high molecular weight material and has very poor tissue penetration capability. For instance, HA can only be dissolved at very
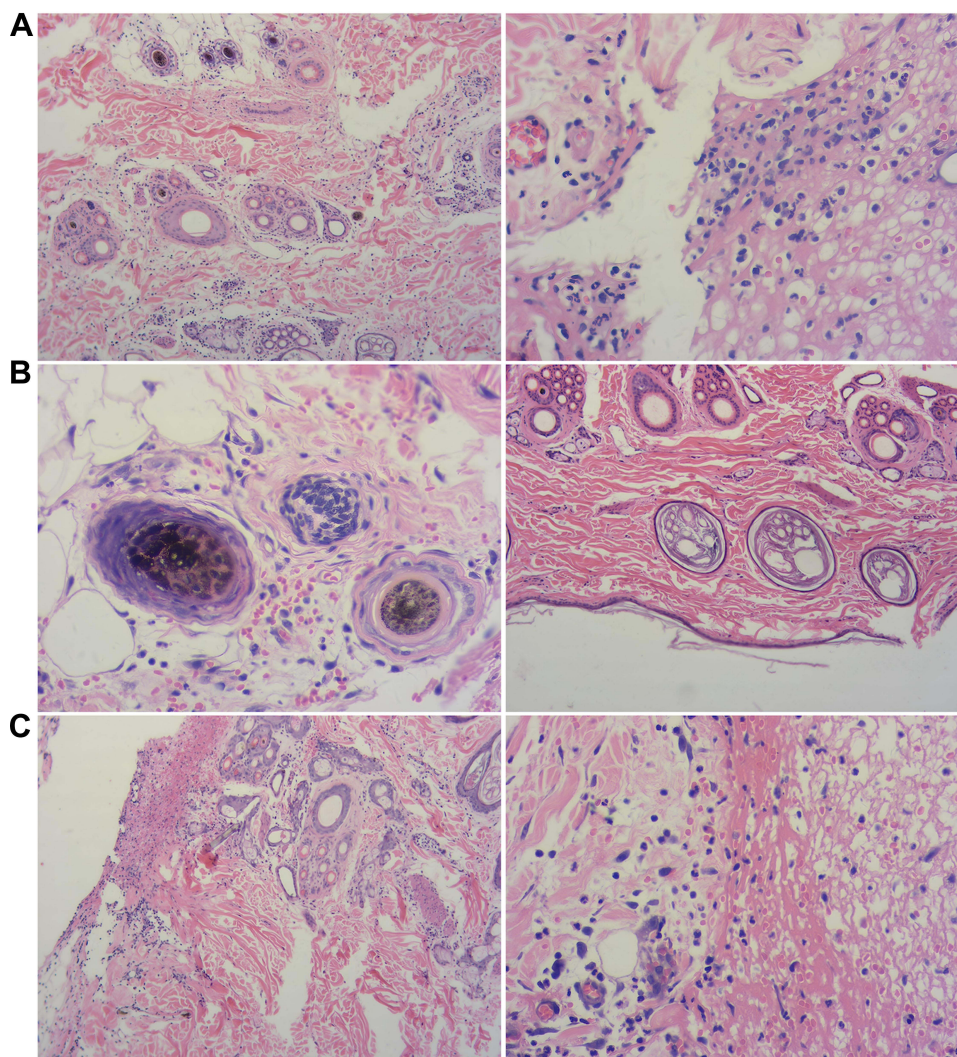
**Figure 7** Observation on tissue sections of B-HA injection on wound inflammation (**A**) Control; (**B**) B-HA; (**C**) HA. (200×). (**A**) Control group: A large number of inflammatory cells infiltrated around the hair follicles and sweat glands in the dermis; a large number of inflammatory cells infiltrated in the wound margin. (**B**) B-HA group: There is a small amount of bleeding around the wound edge, and a small amount of inflammatory cell infiltration around the hair follicle, a very small amount of inflammatory cell infiltration between the connective tissues of the dermis. (**C**) HA group: No inflammatory cell infiltration around the hair follicle, red blood cells and inflammatory cells around the wound margin, but denser; the wound margin is clearly demarcated from normal tissue, and granulation tissue is formed.

low concentration in water-soluble fluids. This property limits its applications only to local injections such as HA joint injection and HA dermal filler. In addition, HA is an acidic mucopolysaccharide with different molecular weights that may have different biological activities. Therefore, novel B-HA assay methods were developed, including a molecular weight distribution assessment using the negative correlation between the molecular weight of B-HA and the percent concentration that induced erythrocyte aggregation (rouleaux formation) and a quality control assessment of B-HA products among batches using elevated erythrocyte sedimentation rates.

The results of previous studies indicated that 35 kDa HA fragments could easily pass through a filter with a pore size of 220 nanometers, indicating its great tissue penetration capability as well as cell surface CD44 binding capability. Our previous results also indicated that 35 kDa HA fragments could be stably generated by the digestion using a recombinant human hyaluronidase PH20 for a period of incubation between 15 minutes and 5 hours at 37 °C.[69] Interestingly, they all generated 35 kDa HA fragments. By balancing between tissue penetration and cell surface CD44 binding capability, this study choses 3.5kDa HA fragments to serve as the injection raw material for clinical use.

A low concentration (40 µg/mL) of 35 kDa B-HA inhibited the production of ROS by human neutrophils. High concentration (300 µg/mL) of 35 kDa B-HA promoted the migration of freshly extracted human monocytes, suggesting that B-HA and the

water it carries can be absorbed from inflamed tissues into the lymphatic system for reflux together with human monocytes. In addition, high concentrations of B-HA significantly inhibited neutrophil migration in the presence or absence of LPS, suggesting that the use of higher concentrations of B-HA in local tissues has an antiinflammatory effect. After the injection of 35 kDa B-HA, it can rapidly enter the spleen through the lymph. B-HA in the blood was rapidly absorbed by tissues, such as the lungs, or was metabolized.

Although the physiological and pharmacological significance of B-HA-induced erythrocyte aggregation (rouleaux formation) and accelerated erythrocyte sedimentation rate in humans are still not clear, relevant literature indicates that HA indirectly affects leukocyte trafficking and leukocyte activation via the erythrocyte and erythroid receptor CD44 and the leukocyte receptor Siglec-9.[31–33] Consequently, these intravascular erythrocyte-related changes could potentially be attributed to the role of intravascular neutrophils in the formation of axial flow and adsorption on the vascular surface and binding to the HA receptor Siglec-9.[57,58] In addition, relevant literature also indicates that the high expression of the macromolecular HA gene results in a decrease in ROS levels in bone marrow hematopoietic stem cells.[70] ROS effectively degrade macromolecular HA and produce HA fragments.[71] In this study, low concentrations of 35 kDa B-HA (40 μg/mL) and 1600 kDa HA (40 μg/mL) both inhibited PMA-induced ROS production by human neutrophils (Figure 5A). Therefore, HA and B-HA reduce ROS levels through the attraction and consumption of ROS. The results of this study suggest that HA and B-HA have identical affinity for or inhibit, to the same degree, the activated human leukocyte receptors CD44, LYVE-1 or Siglec-9. This study showed that high concentrations (300 μg/mL) of B-HA, HA and the combination of B-HA and HA inhibited the migration of human neutrophils in the presence or absence of the endotoxin LPS (Figure 5B and C). Dexamethasone also had an inhibitory effect on neutrophil migration (unpublished data). Results from our previous studies indicated that commercial products containing high concentrations of 1–2% (10–20 mg/mL) B-HA were effective for the treatment of localized inflammatory redness, swelling, fever, and pain in the skin and mucous membrane of the pharynx.[18–23] Thus, the topical application of high concentrations of B-HA to the skin mucosa has therapeutic effects on inflammatory redness, swelling, fever, and pain in the skin mucous membrane, further supporting the physiological phenomenon that few neutrophils are found in the lymphatic system, where the HA concentration is high (Figure 5B and C). In addition, relevant literature reports that the contents of HA and HA fragments in central nervous tissue were at least 330–1150 times higher than those in serum tissue (33–115/0.01 μg/g-0.1 μg/g tissues), suggesting that a high concentration of 35 kDa B-HA also plays a role in brain tissues.[1]

Tissue distribution studies of $^{99m}$Tc-B-HA in mice revealed the tissue distribution and blood half-life of B-HA. HA and HA fragments are at least 85–180 times higher in the chest lymph nodes and lacteal vessels of the thymus than in serum tissues (8.5–18.0/0.01 μg/0.1 μg/g tissue),[1] suggesting high concentrations of HA and HA fragments in the lymphatic system. Recent studies have also demonstrated that in each adult, 10–100 mg of HA and HA fragments enters the blood through the lymphatic system every day.[1–3,48–50] Similarly to HA, B-HA carries water to promote the reabsorption of extracellular fluid in inflammatory tissues. Combined with fluorescent labeling experiments, high concentrations of B-HA accelerate the patrolling of mononuclear cells in the lymphatic system in vivo and the homing of mononuclear cells (mainly lymphocytes and a small amount of macrophage precursors, namely monocytes), namely return to blood circulation through lymphatic vessels. The canine skin experiment showed that compared with the control group, there was a small amount of bleeding around the wound edge, a small amount of inflammatory cell infiltration around the hair follicles, and a very small amount of inflammatory cell infiltration between the dermal connective tissues. Related studies report that the inflammation of skin and mucous membranes with clinical manifestations of redness, swelling, fever, and pain resolved through the effect of lymphatic reflux,[1,9,10,12–23,50,61] which was consistent with the results of promoting monocyte migration.

## Conclusion

Overall, the 35kDa HA fragments has the potential to be effective drugs for the clinical treatment of pain, redness, swelling, inflammatory pain, and inflammatory diseases,[8–10,12–18,51,61] may regulate tumor immunity and be used to treat tumors,[19–23] and may also play an important role in the treatment and prevention of cardiovascular and cerebrovascular diseases.[24,25] Furthermore, the findings of this study and the related literatures suggest that the clinical effects of injectable 35 kDa B-HA in humans are the result of B-HA binding to multiple receptors in different cells, tissues, and organs, supporting the need for further high-dose animal studies or direct human studies of the comprehensive clinical effects.

## Acknowledgment

We would like to thank Harrison Barrett and Professor Lars Furenlid of the University of Arizona for their technical support. iQID dynamic imaging of the whole-body distribution of $^{99m}$Tc-B-HA in mice was conducted at the Center for Gamma-Ray Imaging, University of Arizona, USA. This center is supported by the research grant NIH/NIBIB P41-EB002035 (USA).

## Disclosure

The authors report no conflicts of interest in this work.

## References

1. Jackson DG. Hyaluronan in the lymphatics: the key role of the hyaluronan receptor LYVE-1 in leucocyte trafficking. *Matrix Biol.* 2019;78–79:219–235. doi:10.1016/j.matbio.2018.02.001
2. McDonald B, Kubes P. Interactions between CD44 and hyaluronan in leukocyte trafficking. *Front Immunol.* 2015;6:68. doi:10.3389/fimmu.2015.00068
3. Jackson DG. Leucocyte trafficking via the lymphatic vasculature— mechanisms and consequences. *Front Immunol.* 2019;10:471. doi:10.3389/fimmu.2019.00471
4. Zamboni F, Wong CK, Collins MN. Hyaluronic acid association with bacterial, fungal and viral infections: can hyaluronic acid be used as an antimicrobial polymer for biomedical and pharmaceutical applications? *Bioact Mater.* 2023;19:458–473. doi:10.1016/j.bioactmat.2022.04.023
5. Quero L, Klawitter M, Schmaus A, et al. Hyaluronic acid fragments enhance the inflammatory and catabolic response in human intervertebral disc cells through modulation of toll-like receptor 2 signalling pathways. *Arthritis Res Ther.* 2013;154:1–13. doi:10.1186/ar4274
6. Winters C, Zamboni F, Beaucamp A, Culebras M, Collins MN. Synthesis of conductive polymeric nanoparticles with hyaluronic acid based bioactive stabilizers for biomedical applications. *Mater Today Chem.* 2022;25:100969. doi:10.1016/j.mtchem.2022.100969
7. Zamboni F, Okoroafor C, Ryan MP, et al. On the bacteriostatic activity of hyaluronic acid composite films. *Carbohydr Polym.* 2021;260:117803. doi:10.1016/j.carbpol.2021.117803
8. Valachova K, Svik K, Biro C, et al. Impact of ergothioneine, hercynine, and histidine on oxidative degradation of hyaluronan and wound healing. *Polymers.* 2020;13(1):95. doi:10.3390/polym13010095
9. Fraser JRE, Laurent TC, Laurent UBG. Hyaluronan: its nature, distribution, functions and turnover. *Intern Med J.* 1997;242(1):27–33. doi:10.1046/j.1365-2796.1997.00170.x
10. Lena L. Clearance of hyaluronan from the circulation. *Adv Drug Deliv Rev.* 1991;7:221–235. doi:10.1016/0169-409X(91)90003-U
11. Phillipson M, Kubes P. The neutrophil in vascular inflammation. *Nat Public Health Emergen Collect.* 2011;17(11):1381–1390. doi:10.1038/nm.2514
12. Tengblad A, Laurent UBG, Lilja K, et al. Concentration and relative molecular mass of hyaluronate in lymph and blood. *Biochem J.* 1986;236(2):521–525. doi:10.1042/bj2360521
13. Fraser JR, Kimpton WG, Laurent TC, et al. Uptake and degradation of hyaluronan in lymphatic tissue. *Biochem J.* 1988;256(1):153. doi:10.1042/bj2560153
14. Reed RK, Laurent UB, Fraser JR, et al. Removal rate of [3H]hyaluronan injected subcutaneously in rabbits. *Am J Physiol Heart Circ Physiol.* 1990;259(2):H532–H535. doi:10.1152/ajpheart.1990.259.2.H532
15. Ji RR, Chamessian A, Zhang YQ. Pain regulation by non-neuronal cells and inflammation. *Science.* 2016;354(6312):572–577. doi:10.1126/science.aaf8924
16. Chen G, Zhang YQ, Qadri YJ, et al. Microglia in pain: detrimental and protective roles in pathogenesis and resolution of pain. *Neuron.* 2018;100(6):1292–1311. doi:10.1016/j.neuron.2018.11.009
17. Haight ES, Forman TE, Cordonnier SA, et al. Microglial modulation as a target for chronic pain: from the bench to the bedside and back. *Anesth Analg.* 2019;128(4):737–746. doi:10.1213/ANE.0000000000004033
18. Wang MJ, Kuo JS, Lee WW, et al. Translational event mediates differential production of tumor necrosis factor-alpha in hyaluronan-stimulated microglia and macrophages. *J Neurochem.* 2006;97(3):857–871. doi:10.1111/j.1471-4159.2006.03776.x
19. Austin JW, Gilchrist C, Fehlings MG. High molecular weight hyaluronan reduces lipopolysaccharide mediated microglial activation. *J Neurochem.* 2012;122(2):344–355. doi:10.1111/j.1471-4159.2012.07789.x
20. Jensen G, Holloway JL, Stabenfeldt SE. Hyaluronic acid biomaterials for central nervous system regenerative medicine. *Cells.* 2020;9(9):2113. doi:10.3390/cell9092113
21. Shen MQ, Liu X, Wei C, et al. Clinical study of 35kDa hyaluronan fragment B-HA on laser-induced inflammatory skin wound. *Prog Mod Bio.* 2015;15(7):1300–1304. doi:10.13241/j.cnki.pmb.2015.07.026
22. Hui MZ. Expert opinion: clinical effect of inflammation control by frozen cold pack, ozonated water and hyaluronan fragment on wound healing. *J Gen Surg.* 2015;3(4):8–11. doi:10.13241/j.cnki.pmb.2015.16.014
23. Zhao HD, Hui MZ. Preliminary study of 35kDa hyaluronan fragment B-HA on chronic pharyngitis. *ClinJ Med Officer.* 2014;42(8):864–867. doi:10.3969/j.issn.1671-3826.2014.08.35
24. Zhao HD, Hui MZ. Preliminary study of 35kDa hyaluronan fragment B-HA on laryngopharyngeal reflux disease. *J Clin Med Liter.* 2016;3(24):4898–4899.
25. Zhang HW, Wei WR, Cheng XF, et al. Study on the control effect of bioactive hyaluronic acid B-HA toothpaste on adolescent gingivitis. *Med J Air Force.* 2020;36(1):71–73. doi:10.3969/j.issn.2095-3402.2020.01.021
26. Huang PF, Feng P, Shuang B, et al. Clinical study of 35kDa hyaluronan fragment B-HA tooth brush gel on puberty gingivitis. *Med J Air Force.* 2020;36(1):71–74. doi:10.3969/j.issn.2095-3402.2020.01.021

27. Chanmee T, Ontong P, Itano N. Hyaluronan: a modulator of the tumor microenvironment. *Cancer Lett*. 2016;375(1):20–30. doi:10.1016/j. canlet.2016.02.031

28. Turley EA, Wood DK, McCarthy JB. Carcinoma cell hyaluronan as a "Portable" cancerized prometastatic microenvironment. *Cancer Res*. 2016;76 (9):2507–2512. doi:10.1158/0008-5472.CAN-15-3114

29. Kuang DM, Wu Y, Chen N, et al. Tumor-derived hyaluronan induces formation of immunosuppressive macrophages through transient early activation of monocytes. *Blood*. 2007;110(2):587–595. doi:10.1182/blood-2007-01-068031

30. Zhang G, Guo L, Yang C, et al. A novel role of breast cancer-derived hyaluronan on inducement of M2-like tumor-associated macrophages formation. *Oncoimmunology*. 2016;5(6):e1172154. doi:10.1080/2162402X.2016.1172154

31. Kobayashi N, Miyoshi S, Mikami T, et al. Hyaluronan deficiency in tumor stroma impairs macrophage trafficking and tumor neovascularization. *Cancer Res*. 2010;70(18):7073–7083. doi:10.1158/0008-5472.CAN-09-4687

32. Lim HY, Lim SY, Tan CK, et al. Hyaluronan Receptor LYVE-1-expressing macrophages maintain arterial tone through hyaluronan-mediated regulation of smooth muscle cell collagen. *Immunity*. 2018;49(2):326–341. doi:10.1016/j.immuni.2018.06.008

33. Wang N, Liu C, Wang X, et al. Hyaluronic acid oligosaccharides improve myocardial function reconstruction and angiogenesis against myocardial infarction by regulation of macrophages. *Theranostics*. 2019;9(7):1980–1992. doi:10.7150/thno.31073

34. Kerfoot SM, McRae K, Lam F, et al. A novel mechanism of erythrocyte capture from circulation in humans. *Exp Hematol*. 2008;36(2):111–118. doi:10.1016/j.exphem.2007.08.029

35. Seluanov A, Gladyshev VN, Vijg J, et al. Mechanisms of cancer resistance in long-lived mammals. *Nat Rev Cancer*. 2018;18(7):433–441. doi:10.1038/s41568-018-0004-9

36. Tian X, Azpurua J, Hine C, et al. High-molecular-mass hyaluronan mediates the cancer resistance of the naked mole rat. *Nature*. 2013;499 (7458):346–349. doi:10.1038/nature12234

37. Takasugi M, Firsanov D, Tombline G, et al. Naked mole-rat very-high-molecular-mass hyaluronan exhibits superior cytoprotective properties. *Nat Commun*. 2020;11(1):2376. doi:10.1038/s41467-020-16050-w

38. Cowman MK, Lee HG, Schwertfeger KL, et al. the content and size of hyaluronan in biological fluids and tissues. *Front Immunol*. 2015;6:261. doi:10.3389/fimmu.2015.00261

39. Kobayashi T, Chanmee T, Itano N. Hyaluronan: metabolism and function. *Biomolecules*. 2020;10(11):1525. doi:10.3390/biom10111525

40. Chowdhury B, Hemming R, Hombach-Klonisch S, et al. Murine hyaluronidase 2 deficiency results in extracellular hyaluronan accumulation and severe cardiopulmonary dysfunction. *J Biol Chem*. 2013;288(1):520–528. doi:10.1074/jbc.M112.393629

41. Chowdhury B, Xiang B, Muggenthaler M, et al. Hyaluronidase 2 deficiency is a molecular cause of cor triatriatum sinister in mice. *Int J Cardiol*. 2016;209:281–283. doi:10.1016/j.ijcard.2016.02.072

42. Chowdhury B, Xiang B, Liu M, et al. Hyaluronidase 2 deficiency causes increased mesenchymal cells, congenital heart defects, and heart failure. *Circ Cardiovasc Genet*. 2017;10(1):e001598. doi:10.1161/CIRCGENETICS.116.001598

43. Matsumoto K, Li Y, Jakuba C, et al. Conditional inactivation of Has2 reveals a crucial role for hyaluronan in skeletal growth, patterning, chondrocyte maturation and joint formation in the developing limb. *Development*. 2009;136(16):2825–2835. doi:10.1242/dev.038505

44. Huang Y, Askew EB, Knudson CB, et al. CRISPR/Cas9 knockout of HAS2 in rat chondrosarcoma chondrocytes demonstrates the requirement of hyaluronan for aggrecan retention. *Matrix Biol*. 2016;56:74–94. doi:10.1016/j.matbio.2016.04.002

45. Hunnicutt GR, Primakoff P, Myles DG. Sperm surface protein PH-20 is bifunctional: one activity is a hyaluronidase and a second, distinct activity is required in secondary sperm-zona binding. *Biol Reprod*. 1996;55:80–86. doi:10.1095/biolreprod55.1.80

46. Locke KW, Maneval DC, LaBarre MJ. ENHANZE® drug delivery technology: a novel approach to subcutaneous administration using recombinant human hyaluronidase PH20. *Drug Deliv*. 2019;26(1):98–106. doi:10.1080/10717544.2018.1551442

47. Beech DJ, Madan AK, Deng N. Expression of PH-20 in normal and neoplastic breast tissue. *J Surg Res*. 2002;103:203–207. doi:10.1006/jsre.2002.6351

48. Printz MA, Dychter SS, DeNoia EP. A Phase I study to evaluate the safety, tolerability, pharmacokinetics, and pharmacodynamics of recombinant human hyaluronidase PH20 administered intravenously in healthy volunteers. *Curr Ther Res*. 2020;19:100604. doi:10.1016/j.curtheres.2020.100604

49. Shimoda M, Yoshida H, Mizuno S, et al. Hyaluronan-binding protein involved in hyaluronan depolymerization controls endochondral ossification through hyaluronan metabolism. *Am J Pathol*. 2017;187(5):1162–1176. doi:10.1016/j.ajpath.2017.01.005

50. Homann S, Grandoch M, Kiene LS, et al. Hyaluronan synthase 3 promotes plaque inflammation and atheroprogression. *Matrix Biol*. 2018;66:67–80. doi:10.1016/j.matbio.2017.09.005

51. Bahrami SB, Tolg C, Peart T, et al. Receptor for hyaluronan mediated motility (RHAMM/HMMR) is a novel target for promoting subcutaneous adipogenesis. *Integr Biol*. 2017;9(3):223–237. doi:10.1039/c7ib00002b

52. Jia Q, Wu H, Zhou X, et al. A "GC-rich" method for mammalian gene expression: a dominant role of non-coding DNA GC content in regulation of mammalian gene expression. *Sci China Life Sci*. 2010;53(1):94–100. doi:10.1007/s11427-010-0003-x

53. Hill DR, Kessler SP, Rho HK, et al. Specific-sized hyaluronan fragments promote expression of human beta-defensin 2 in intestinal epithelium. *J Biol Chem*. 2013;287(36):30610–30624. doi:10.1074/jbc.M112.356238

54. Rl HD, Rho HK, Kessler SP, et al. Human milk hyaluronan enhances innate defense of the intestinal epithelium. *J Biol Chem*. 2013;288(40):29090. doi:10.1074/jbc.M113.468629

55. Kessler SP, Obery DR, Nickerson KP, et al. Multifunctional role of 35 kilodalton hyaluronan in promoting defense of the intestinal epithelium. *J Histochem Cytochem*. 2018;66(4):273–287. doi:10.1369/0022155417746775

56. Kim Y, Kessler SP, OberyD R, et al. Hyaluronan 35kDa treatment protects mice from citrobacter rodentium in fection and induces epithelial tight junctional protein ZO-1 in vivo. *Matrix Biology*. 2017;62:28–39. doi:10.1016/j.matbio.2016.11.001

57. Gunasekaran A, Eckert J, Burge K, et al. Hyaluronan 35kDa enhances epithelial barrier function and protects against the development of murine necrotizing enterocolitis. *Pediatr Res*. 2019;87(7):1177–1184. doi:10.1038/s41390-019-0563-9

58. Luquita A, Urli L, Svetaz MJ, et al. In vitro and ex vivo effect of hyaluronic acid on erythrocyte flow properties. *J Biomed Sci*. 2010;17(1):8. doi:10.1186/1423-0127-17-8

59. Melder RJ, Yuan J, Munn LL, et al. Erythrocytes enhance lymphocyte rolling and arrest in vivo. *Microvasc Res*. 2000;59(2):316–322. doi:10.1006/mvre.1999.2223

60. Laznicek M, Laznickova A, Cozikova D, Velebny V. Preclinical pharmacokinetics of radiolabelled hyaluronan. *Pharmacol Rep*. 2012;64 (2):428–437. doi:10.1016/s1734-1140(12

61. Huang C, Chen F, Zhang L, Yang Y, Yang X, Pan W. (99m)Tc Radiolabeled HA/TPGS-based curcumin-loaded nanoparticle for breast cancer synergistic theranostics: design, in vitro and in vivo evaluation. *Int J Nanomedicine*. 2020;15:2987–2998. doi:10.2147/IJN.S242490

62. Laurent UBG, Reed RK. Turnover of hyaluronan in the tissues. *Adv Drug Deliv Rev*. 1991;7(2):237–256. doi:10.1016/0169-409X(91

63. Lazcano-Silveira R, Jia X, Liu K, Liu H, Xinrong L, Hui M. Carbon 60 dissolved in grapeseed oil inhibits dextran sodium sulfate-induced experimental colitis. *J Inflamm Res*. 2022;15:4185–4198. doi:10.2147/JIR.S366886

64. Secundino I, Lizcano A, Roupé KM, et al. Host and pathogen hyaluronan signal through human siglec-9 to suppress neutrophil activation. *J Mol Med*. 2016;94(2):219–233. doi:10.1007/s00109-015-1341-8

65. Lizcano A, Secundino I, Döhrmann S, et al. Erythrocyte sialoglycoproteins engage Siglec-9 on neutrophils to suppress activation. *Blood*. 2017;129 (23):3100–3110. doi:10.1182/blood-2016-11-751636

66. Kiser ZM, Lizcano A, Nguyen J, et al. Decreased erythrocyte binding of Siglec-9 increases neutrophil activation in sickle cell disease. *Blood Cells Mol Dis*. 2020;81:102399. doi:10.1016/j.bcmd.2019.102399

67. Smith ES, Omerbašić D, Lechner SG, et al. The molecular basis of acid insensitivity in the African naked mole-rat. *Science*. 2011;334 (6062):1557–1560. doi:10.1126/science.1213760

68. Kulaberoglu Y, Bhushan B, Hadi F, et al. The material properties of naked mole-rat hyaluronan. *Sci Rep*. 2019;9(1):6632. doi:10.1038/s41598-019-43194-7

69. Jia X, Tong H, Li X, Jiayou C, Hui M. A method to produce 35kDa hyaluronan fragment and its application. *Chinese and PCT Patent No*.2021102700130; 2021.

70. Ke ZH. *Stem Cell Maintenance in Naked Mole Rats and Other Longevity Mechanisms in Rodents*. University of Rochester ProQuest Dissertations Publishing; 2018:10750894.

71. Šoltés L, Mendichi R, Kogan G, et al. Degradative action of reactive oxygen species on hyaluronan. *Biomacromolecules*. 2006;(3):659–668. doi:10.1021/bm050867v